Journal of Applied Polymer Science

Development, rheological properties, and physical stability of D-limonene-in-water emulsions formulated with copolymers as emulsifiers

Luis A. Trujillo-Cayado, M. Carmen García, José Muñoz, M. Carmen Alfaro
Reología Aplicada, Tecnología De Coloides, Departamento De Ingeniería Química, Facultad De Química, Universidad De Sevilla C/P. García González, Sevilla E41012, Spain
Correspondence to: M. C. A. Rodríguez (E-mail: alfaro@us.es)

ABSTRACT: This contribution reports the development of 30 wt % D-limonene-in-water emulsions formulated with a biopolymer (gellan gum) as stabilizer and prepared with a high-pressure homogenizer. The role as emulsifiers of different ratios of amphiphilic copolymers (Atlas™ G5000 and Atlox™ 4913) was assessed. The results indicated that the ratio of emulsifiers had significant effect on the physical stability, droplet size, viscoelasticity, and viscosity of these emulsions. The mean droplet diameters decreased as Atlas™ G5000 concentration increased from 1 wt % to 3 wt %. The aging of emulsions resulted in an increase in the size of droplets for the emulsions containing high Atlox™ 4913 copolymer content. An increase of Atlas™ G5000 enhanced both the G' and G'' values and the viscosity providing higher stability to emulsions. Gellan gum caused in viscoelastic moduli weaker frequency dependence at the lower frequencies, according to the formation of a faint gel-like matrix. All emulsions exhibited shear thinning flow properties that fitted the power-law equation. © 2016 Wiley Periodicals, Inc. J. Appl. Polym. Sci. **2016**, *133*, 43838.

KEYWORDS: colloids; copolymers; rheology

Received 20 October 2015; accepted 27 April 2016
DOI: 10.1002/app.43838

INTRODUCTION

Oil-in-water emulsions are thermodynamically unstable systems in which oil is dispersed in aqueous phase. They tend to separate into two layers over time through some physicochemical mechanisms such as creaming, coalescence, flocculation, and/or Ostwald ripening.[1] The use of surfactants and/or thickeners is essential with a view to improve the stability of emulsion.[2]

Regarding the oil phase it should be noted that nowadays, there is a growing interest by essential oils. They have interesting antimicrobial and antioxidant properties which provoke that recently several authors have performed a great effort to investigate their use in diverse application fields such as food, pharmaceutical, and the agrochemical industry.[3–5] This work deals with the development of emulsions containing D-limonene as disperse phase. D-Limonene is an interesting biosolvent that can be obtained from citric peels. It exhibits good biodegradability according to the requirement to meet the ever-increasing safety and environmental demands of the 21st Century.[6] Given that D-limonene is not soluble in water, emulsification is an interesting alternative to solubilize and protect D-limonene from oxidative degradation.[7]

Two amphiphilic copolymers have been used in order to emulsify D-limonene. These surfactants have an indispensable role in the formation and stabilization of emulsions.[8] In this article, the use of Atlas™ G-5000 hydrophilic copolymer (HLB = 16.9) and the Atlox™ 4913 amphiphilic copolymer (HLB about 11–12) as emulsifiers will be investigated. This latter polymeric surfactant is composed of a main chain of methyl methacrylate (PMMA) as an anchor fraction and polyethylenglycol chains (PEG) of suitable length as a stabilizer fraction. Atlas™ G-5000 hydrophobic chains, poly-B block of poly(propylene oxide), work as anchoring groups in the organic phase while the hydrophilic chain, poly-A block of poly(ethylene oxide), ensures the stability of the external aqueous phase.

Polysaccharides are widely used as thickening, stabilizing, and emulsifying agents for their biocompatibility, biodegradability, and non-toxicity. Although gellan gum possesses a great practical potential, it is a biopolymer seldom used in these purposes.[9–12] In an emulsion containing a thickening agent such gellan gum, creaming is strongly inhibited due to the immobilization of droplets in a weak gel-like polymer network having a very high zero-shear viscosity value in comparison with emulsions formulated in the absence of thickening agents.[13]

The most common emulsification methods are based on mechanical energy input to the system by an external source. As a rule, emulsions are prepared in two steps. The aim of the first step (primary homogenization) is to create droplets of dispersed phase such that a coarse emulsion is formed. This step is usually carried out by means of a rotor/stator system. The goal of the second step is to reduce the size of pre-existing droplets to a submicron level, which usually involves the use of a different homogenizer, such as ultrasonic probes, high-pressure valve homogenizers, or microfluidizers.[14,15] High-pressure homogenizers are the most important continuously operated emulsifying devices used in industry to produce finely dispersed emulsions.[16]

The main objective of this work was to study the influence of the amphiphilic copolymer mass ratio (Atlas™ G-5000 and Atlox™ 4913) as emulsifier on the rheological properties, droplet size distribution, and physical stability of D-limonene/W emulsions developed using a high-pressure homogenizer and formulated with a microbial gum.

EXPERIMENTAL

Materials

The organic solvent used was rectified D-limonene, which was supplied by Destilaciones Bordas-Chinchurreta Company (Sevilla, Spain). The D-limonene concentration was fixed to 30 wt %.

Two types of amphiphilic copolymers were used as emulsifiers, which may be considered to be polymeric surfactants.[12] Atlas™ G-5000 (hydrophilic AB block copolymer) and Atlox™ 4913 (grafted copolymer) surfactants were supplied by Commercial Química Massó Company (Barcelona, Spain). The total concentration of copolymers was 3.0 wt %, although the ratio Atlas™ G-5000 to Atlox™4913 was varied: 3/0, 2.5/0.5, 2/1, 1/2, and 0/3. The nomenclature used to denote the composition of emulsions is as follows: *X*/*Y* stands for emulsions containing *X* wt % Atlas™ G-5000 and *Y* wt % Atlox™ 4913.

Commercial low-acyl gellan gum, Kelcogel F type was used as stabilizer as supplied by CP Kelco Company (San Diego, CA). The total concentration of gellan gum in the emulsions was 0.4 wt %. In order to prevent the growth of microorganisms, 0.1 wt % sodium azide was added to the final formulation.

Methods

Emulsification Process. In the preparation of gum solutions and emulsions studied, the protocols utilized in a previous study were used.[4] These protocols consist of the following consecutive steps.

First, the gum solutions were prepared by slowly dispersing 0.8 wt % gellan gum in deionized water at room temperature. Subsequently, they were mechanically stirred using an IKA-Visc MR-D1 in combination with a Saw-tooth type rotor in a bath at 80 °C in order to facilitate their hydration. Finally, the water lost due to evaporation during the dispersion and hydration steps was replaced.

Second, oil-in-water emulsions were produced in two steps: In the first step, coarse emulsions were prepared with an Ultraturrax T-50/G45F rotor-stator device by applying a rotational speed of 4000 rpm for 120 s at room temperature. Atlas™ G-5000 and Atlox™ 4913 were dispersed in the corresponding amount of water. Afterwards, D-limonene was added slowly to the aqueous one while the system was agitated using the aforementioned homogenizer. The pre-emulsion was passed through a high-pressure valve homogenizer (Avestin EmulsiFlex-C5 type) three times at 1500 psi (10.3 MPa). Finally, this emulsion was mixed with an equal amount of a solution of hydrocolloid. For this purpose, the Ultra-Turrax T-50 was used.

Oscillatoy Shear Tests. Stress sweeps were performed in a range of 0.05–3 Pa at three different frequencies: 0.1 Hz, 1 Hz, and 3 Hz. Frequency sweep tests were performed by selecting a stress within the linear range for three previously studied frequencies. A controlled-stress rheometer AR2000 with a serrated plate–plate sensor (40 mm diameter, gap: 1 mm) was used. Equilibration time prior to rheological tests was 10 min. These rheological measurements were carried out at 20 °C ± 0.1 °C, using a Peltier system for sample temperature control. The samples were loaded into the rheometer measurement cell and allowed to equilibrate for 600 s before beginning the test, to allow for stress relaxation. The results represent the mean of, at least, three measurements done on emulsions aged for 24 h.

Steady Shear Flow Tests. The flow tests were carried out using a rheometer from Haake Thermo Scientific (Karlsruhe, Germany), a Mars controlled stress rheometer with a Vane FL40 sensor system ($R_i = 20$ mm, $R_a = 21.70$ mm, $H = 55$ mm). Three different segments have been used to provide a greater number of points along the flow curve: (1) From 0.1 to 1 Pa; (2) From 1.1 to 10 Pa; (3) From 12.5 to 60 Pa. These rheological measurements were performed at 20 °C ± 0.1 °C, using a C5P Phoenix circulator (Thermo-Scientific, Germany) for sample temperature control. The results represent the mean of three measurements.

Droplet Size Distribution. Droplet size distributions of emulsions aged for 1, 2, 5, 14, 28, and 60 days were measured using a static light scattering instrument (Mastersizer X; Malvern Instruments, UK) after samples had been diluted with water.

The mean droplet diameters were expressed as Sauter diameter ($D_{3,2}$) and volume mean diameter ($D_{4,3}$):

$$D_{3,2} = \sum_{i=1}^{N} n_i d_i^3 \Big/ \sum_{i=1}^{N} n_i d_i^2 \quad (1)$$

$$D_{4,3} = \sum_{i=1}^{N} n_i d_i^4 \Big/ \sum_{i=1}^{N} n_i d_i^3 \quad (2)$$

where d_i is the droplet diameter, N is the total number of droplets, and n_i is the number of droplets having a diameter d_i.

Determinations were conducted in triplicate.

Multiple Light Scattering. The destabilization of emulsions was monitored by multiple light scattering using an optical scanning instrument (Turbiscan Lab Expert). Emulsions were placed into cylindrical glass tubes and stored at room temperature. The backscattering of light from emulsions was then measured with height at different times. The results were presented in reference

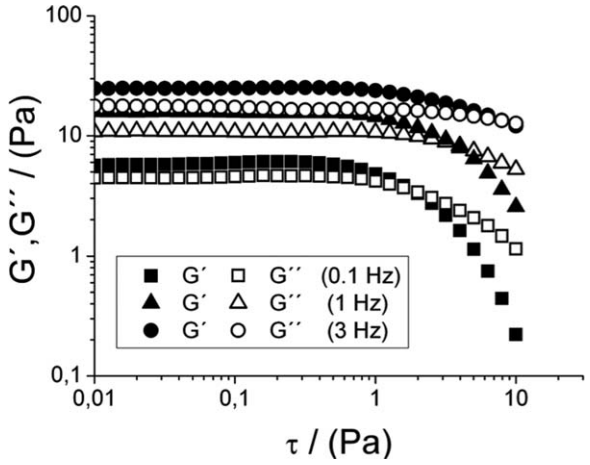

Figure 1. Oscillatory stress sweeps of 30 wt % D-limonene emulsions aged for 24 h for the 3/0 emulsion at 0.1, 1, and 3 Hz. Temperature: 20 °C.

mode (delta-backscattering. ΔBS %), i.e., by subtracting the first scan from all the subsequent scans made.

In order to quantify simultaneously the destabilization processes in the emulsions studied the Turbiscan Stability Index (TSI) was used. This index is a statistical factor and its value is calculated as the sum of all the destabilization processes in the measuring cell and it is given by[17]:

$$\mathrm{TSI}=\sum_j |\mathrm{scan}_{\mathrm{ref}}(h_j)-\mathrm{scan}_i(h_j)| \quad (3)$$

where $\mathrm{scan}_{\mathrm{ref}}$ and scan_i are the initial backscattering value and the backscattering value at a given time, respectively, h_j is a given height in the measuring cell and TSI is the sum of all the scan differences from the bottom to the top of the vial.

Furthermore, one-way analysis of variance (ANOVA) and simple regression analysis were carried out using StatPlus®:mac. All statistical calculations were conducted at a significance level of $P = 0.05$.

RESULTS AND DISCUSSION

Results for 0/3 emulsion are not shown because it was not possible to obtain it with high-pressure homogenizer. By contrast, the coarse emulsion was obtained. For this reason, the energy input must be controlled since over-processing led to the rupture of surfactant interface and thus breaking up of droplets by recoalescence when the Atlox™ 4913 was used alone.

Rheological Measurements

In order to define the upper limit of the linear viscoelastic range (LVR), oscillatory stress sweep tests were conducted. This test was carried out at three different frequencies to ensure that the conditions for linear viscoelastic behavior were fulfilled. In a stress sweep, the storage modulus (G') and the loss modulus (G'') remain practically constant and deformation in the structure is reversible up to a critical stress (τ_c), in which G' and G'' begin to change with increasing stress. The LVR is where the moduli are independent of the applied stress and strain. The value of τ_c reflects the shear resistance of molecular aggregates, when $\tau > \tau_c$, the initial molecular aggregates are disrupted.[18]

Table I. Critical Shear Stress at 0.1 Hz ($\tau_{c,0.1\ \mathrm{Hz}}$), Storage Modulus ($G'$) at the LVR and Loss Modulus (G'') at the LVR Values for All Studied Emulsions

Emulsion	$\tau_{c,0.1\ \mathrm{Hz}}$ (Pa)	G'_{LVR} (Pa)	G''_{LVR} (Pa)
3/0	0.63 ± 0.04	5.56 ± 0.33	4.49 ± 0.31
2.5/0.5	0.50 ± 0.03	4.78 ± 0.28	3.68 ± 0.17
2/1	0.20 ± 0.02	4.05 ± 0.17	3.48 ± 0.18
1/2	0.13 ± 0.01	3.32 ± 0.12	3.13 ± 0.13

Figure 1 shows oscillatory shear stress sweeps as a function of frequency for the emulsion 3/0 by way of example. The onset of non-linear response was detected by a clear fall of G' and G''. It is possible to obtain from these tests the critical stress for the onset of non-linear response. For all studied emulsions, τ_c for 0.1 Hz is more restrictive for the onset of non-linear response than for 1 Hz and 3 Hz ($\tau_{c,0.1\ \mathrm{Hz}} < \tau_{c,1\ \mathrm{Hz}} < \tau_{c,3\ \mathrm{Hz}}$). Critical shear stress values for 0.1 Hz are presented in Table I. The excellent repeatability of the critical shear stress and critical strain supported the consistency of the preparation method used. Results of ANOVA test demonstrated that the LVR at 0.1 Hz is dependent on Atlas™ G-5000/Atlox™ 4913 ratio, since the values of τ_c, G', and G'' steadily went down as the Atlas™ G-5000 concentration was decreased. In addition, for all the studied emulsions G' was greater than G'' at the LVR, as the elastic component dominated the viscous component at 0.1, 1, and 3 Hz.

Figure 2 illustrates the frequency dependence of the linear viscoelastic functions of the studied emulsions to display the influence of surfactants ratio. G' values were slightly higher than those of G'' and the slopes of the linear part of the log–log plot of G' and G'' versus frequency were relatively high. However, at the lower frequencies a clear trend to a weaker influence of frequency was observed. Both viscoelastic functions increased with the Atlas™ G-5000 content. These results indicated the progressive development of a faint gel-like structure as the Atlas™ G-5000/Atlox™ 4913 ratio was increased. This gel must be based on the steric interactions promoted by the hydrated

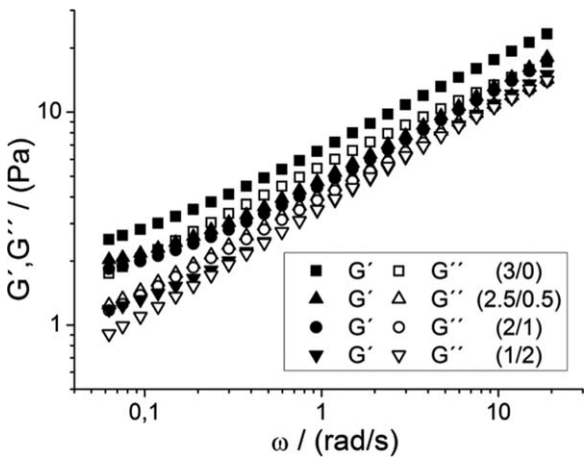

Figure 2. Mechanical spectra of 30 wt % D-limonene emulsions aged for 24 h as a function of the surfactants ratio used as emulsifier. Temperature: 20 °C.

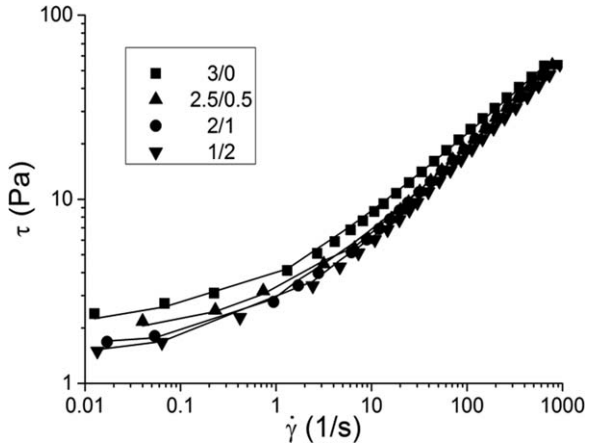

Figure 3. Steady shear flow curves of 30 wt % D-limonene emulsions aged for 24 h as a function of the surfactants ratio. Lines are the best fit to Herschel–Bulkley equation. Temperature: 20 °C.

polyoxyethylene groups of Atlas™ G-5000 with the vital contribution of the biopolymer used. It should be noted that the presence of gellan macromolecules was responsible for the lower frequency dependence observed at low frequency. In other words, gellan gum may form transient junction zones among their macromolecules, justifying the slight trend observed to reach an equilibrium G_e modulus.[10] From a practical point of view, the increasing strength of the faint gel-like structure as Atlas™ G-5000 concentration was greater predicts a better physical stability of the corresponding limonene emulsion. This fact can be attributed to the formation of a semi-permanent network as a consequence of the establishment of hydrogen bonds between the polyoxyethylene groups of Atlas™ G-5000 and water.[12]

Flow curves representing the shear stress dependence on the shear rate for emulsions studied as a function of Atlas™ G-5000/Atlox™ 4913 ratio after one day of aging time are shown in Figure 3. All the emulsions exhibited shear-thinning behaviour so that their viscosity (slope of the plot of stress vs. shear rate) gradually dropped with increasing shear rate. However a deeper observation at low shear rate (see insight in Figure 3) revealed the occurrence of an apparent yield stress. The yield stress of a material can be defined as the minimum shear stress that must be overcome to make a material flow. Namely, below a stress level we observe a solid-like behavior and above this stress level we observe viscous liquid-like behavior. This stress level is the yield stress and it determines the initiation of an emulsion to flow from a container, pumping an emulsion into a transportation pipeline, coating or spreading of an emulsion over a solid substrate.

The occurrence of a yield stress is not unusual since structured fluids such as dense suspensions, colloidal gels, or concentrated emulsions are yield stress fluids. As an example may be mentioned: Crude oil-polymer emulsions,[19] D-limonene/water emulsions prepared with Angum gum,[20] gellan gum fluid gel,[11] or xanthan gum solutions.[21]

The flow curves were successfully fitted to the Herschel–Bulkley equation ($R^2 > 0.999$) in order to identify the flow responses of the emulsion:

$$\tau = \tau_0 + k \cdot \dot{\gamma}^n \quad (4)$$

where τ is the shear stress, τ_0 is the yield stress, k is the consistency index, ($R^2 > 0.999$) is the shear rate and n is the power law index.

Table II shows the values of fitting parameters for the emulsions aged for 24 h as a function of surfactants ratio. Furthermore, the apparent viscosity at a constant shear rate of 0.1 and 100 s^{-1} ($\eta_{0.1}$ and η_{100} respectively) are exhibited, which are calculated as follows:

$$\eta = \frac{\tau}{\dot{\gamma}} \quad (5)$$

Firstly, the non-Newtonian behavior of these emulsions should be noted ($n < 1$).

As can be observed in Table II, the viscosities $\eta_{0.1}$ and η_{100} of these emulsions, which range from 16.10 to 28.97 Pa s and from 0.175 to 0.229 Pa s, respectively, depend on the Atlas™ G-5000/Atlox™ 4913 mass ratio having the Atlas™ G-5000 concentration a big impact on the emulsion viscosity. The 3/0 emulsion exhibited the highest viscosity with values nearly two times higher than 1/2 emulsion. The yield stress, τ_0, ranged from 1.27 to 2.14 Pa and it decreased by increasing the Atlox™ 4913 content, being its value lower than that of emulsions containing higher Atlas™ G-5000 concentration. Atlas™ G-5000 is an emulsifier which is also able to build hydrogen bonds with water. This fact increased the resistance to the flow, which in turn increases the energy need for the flow leading to obtain emulsions with an increasing value both yield stress and viscosity by increasing this copolymer. These results agree with those obtained in mechanical spectra. Regarding the power law index, n, hardly increased with Atlas™ G-5000 content. The results of ANOVA test supported this fact and they demonstrated that Atlas™ G-5000/Atlox™ 4913 mass ratio had no significant effect upon the flow index of the emulsions. By contrast, this test appreciated that this ratio influenced the values of $\eta_{0.1}$, η_{100}, and τ_0.

As expected, in all emulsions $\eta_{0.1}$ values were higher than η_{100} values. This decrease in apparent viscosity by increasing the

Table II. Flow Curves Fitting Parameters for the Herschel–Bulkley Model for Studied Emulsions as a Function of Surfactant Ratio

Emulsion	τ_0 (Pa)	K (Pa)	n	$\tau_{0.1}$ (Pa s)	τ_{100} (Pa s)
3/0	2.14 ± 0.10	2.11 ± 0.07	0.49 ± 0.01	28.97 ± 2.14	0.229 ± 0.018
2.5/0.5	1.92 ± 0.16	1.58 ± 0.05	0.51 ± 0.01	23.37 ± 2.11	0.198 ± 0.018
2/1	1.53 ± 0.13	1.45 ± 0.06	0.52 ± 0.01	19.07 ± 1.52	0.192 ± 0.017
1/2	1.27 ± 0.11	1.39 ± 0.05	0.54 ± 0.01	16.10 ± 1.09	0.175 ± 0.012

Aging time of 24 h.

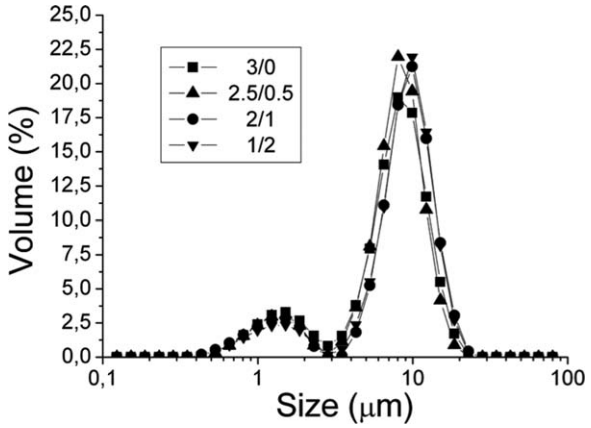

Figure 4. Droplet size distributions for emulsions aged 24 h as a function of the Atlas™ G-5000/Atlox ™ 4913 ratio.

shear rate could be attributed to deformation and breaking of the drop aggregates and their arrangement in the flow field.[1]

Droplet Size Distribution

Figure 4 shows the droplet size distributions of the emulsions aged for 24 h as a function of the Atlas™ G-5000/Atlox™ 4913 ratio. All emulsions showed two populations of droplets and similar droplet size distributions regardless of the surfactant ratio used. The main peak is below 1.5 microns and the second population is located about ten microns. The occurrence of the second population of droplets is probably due to a recoalescence phenomenon of new droplets as a consequence of some over-processing.[22,23] The Sauter and volume mean droplet diameters, $D_{3,2}$ and $D_{4,3}$ respectively, (Figure 5), illustrate that an increase of the content of the Atlox™ 4913 copolymer in the emulsion yielded higher mean diameters and wider droplet size distributions.

These results also support those obtained in flow curves. According to Pal (2000), as droplet size increases, the number of droplets per unit volume of the emulsion decreases and the average distance of separation between the droplets increases.[24]

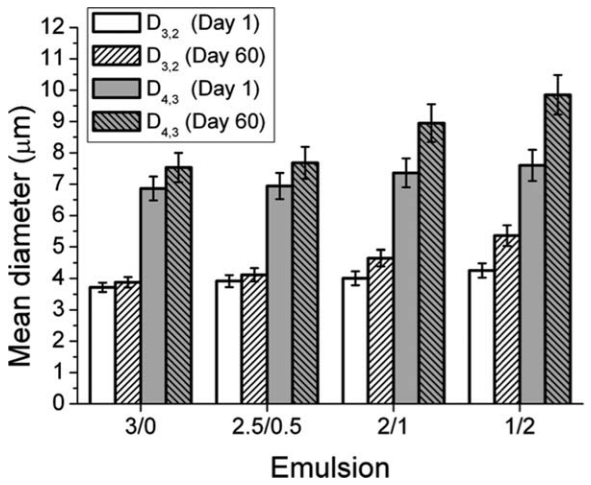

Figure 5. Sauter mean diameter ($D_{3,2}$) and volume mean diameter ($D_{4,3}$) for all the emulsion studied as a function of aging time.

Therefore, the droplets become more mobile and show less resistance to flow showing a lower viscosity.

Regarding aging time (from day 1 to day 60) it should be noted that an increase of the mean diameters occurs (Figure 5). The results obtained pointed out the occurrence of some coalescence for emulsions developed at the range 2–1 wt % of Atlox™ 4913. By contrast, the 3/0 and 2.5/0.5 emulsions did not show any significant changes of droplet sizes.

Multiple Light Scattering

Figure 6 shows by way of the example the delta-backscattering (ΔBS %) profiles obtained as function of time for (a) the 1/2 emulsion and (b) the emulsion containing only Atlas™ G-5000 (3/0). A decrease in backscattering at the bottom of the measuring cell was observed in both samples, which indicated the occurrence of a migration of droplets to the upper part of the cell, i.e., a clarification due to an incipient creaming in this zone of the measurement cell.[25,26] This decrease in backscattering at the lower zone of the tube was observed in all samples. However, the emergence of a destabilization process by creaming was more clearly seen for the emulsions with higher concentrations of Atlox™ 4913 [see Figure 6(A)]. In addition, Figure 6(A) shows a global decrease of backscattering with the aging time in the middle part of the measuring cell. In general, this

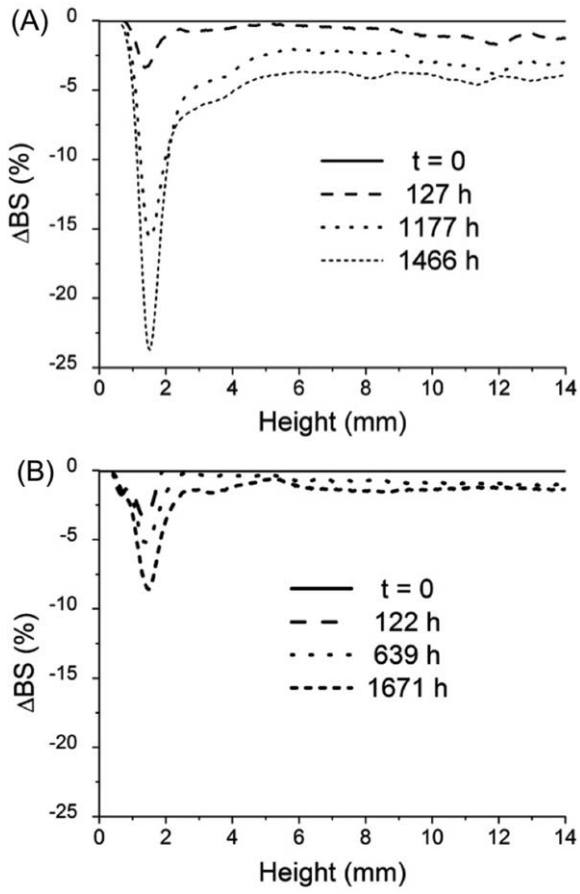

Figure 6. Changes in delta-backscattering profiles as a function of the tube height with the aging time for (A) the 1/2 emulsion and (B) the 3/0 emulsion. Tube length: 55 mm, temperature: 20 °C.

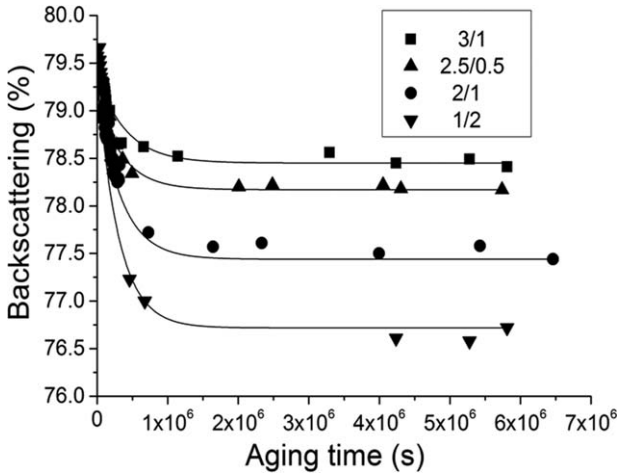

Figure 7. Destabilization kinetic in the 15–20 mm zone monitored over some days for all studied emulsions as a function of the Atlas™ G-5000/Atlox™ 4913 ratio.

evolution can be interpreted as an increase in the emulsion droplet size. To illustrate this behavior the backscattering was fitted to an exponential equation ($R^2 > 0.99$), typically used for a first-order kinetic model[27]:

$$BS = BS_e + (BS_0 - BS_E) \cdot \exp(k \cdot t) \quad (6)$$

where BS stands for backscattering as a function of aging time, BS_E is the corresponding equilibrium value, BS_0 is the initial value of backscattering and k is the first-order kinetic coefficient. To be more precise, the average value of the backscattering (BS) measurement at the central zone of the cell (between 15 and 20 mm of sample height) has been plotted as a function of ageing time (Figure 7). This kinetic equation has proven useful to monitor the physical stability of an emulsion formulated with polymer surfactants as emulsifiers and polysaccharides as stabilizers.[4,12] Table III lists the values of eq. (6) parameters as a function of copolymer concentration. As can be seen, BS_0 decreased as Atlas™ G-5000 concentration was reduced. This result can be attributed to the fact that the lower Sauter mean droplet diameters (higher Atlas™ G-5000 concentration, see Figure 5) result in higher specific surfaces. The first-order kinetic coefficient (k) exhibited a tendency to increase with the rise of the relative concentration of Atlox™ 4913. This fact indicates that the kinetics of coalescence slowed down as an increasing number of molecules of Atlas™ G-5000 accumulated around the limonene/water interface.

Table III. Fitting Parameters of the First-Order Kinetic Equation for the BS in the 15–20 mm Zone of the Measuring Cell versus Aging Time as a Function of Copolymer Concentration

Emulsion	B_{00} (%)	$(BS_0 - BS_E)$ (%)	k (s^{-1})
3/0	78.45	0.93	2.83×10^{-6}
2.5/0.5	78.17	1.01	2.84×10^{-6}
2/1	77.44	1.78	2.98×10^{-6}
1/2	76.72	2.65	3.33×10^{-6}

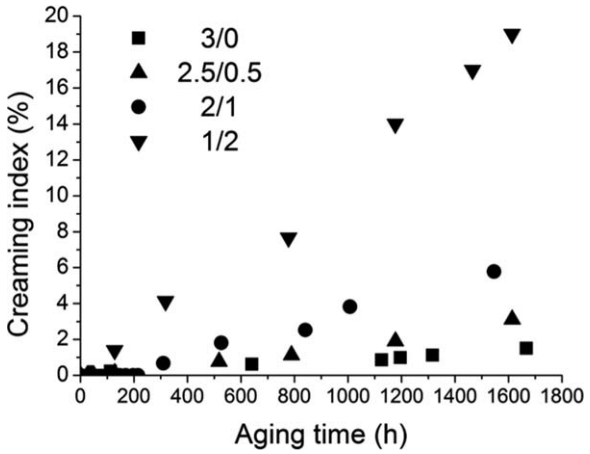

Figure 8. Creaming index (CI) as a function of aging time for all emulsions studied. Samples kept under storage at 20 °C.

The destabilization by creaming of the emulsions was studied using the creaming index (CI), which is defined as[1]:

$$CI(\%) = \frac{H_S}{H_E} \cdot 100 \quad (7)$$

where H_E is the total height of the emulsion and H_S is the height of the serum layer.

In Figure 8, the creaming index (CI) is plotted as a function of aging time for all emulsions. Obviously, the value of the creaming index will depend on the time that the measurement is made. The initial slope of the plot of CI versus time [$d(CI)/d(t)$] is related to the creaming velocity:

$$\omega = \frac{d(CI)}{dt} \cdot \frac{H_E}{100} \quad (8)$$

It was found that the creaming velocity was influenced by the surfactants ratio (Table III). This parameter increases as the Atlas™ G-5000 content decreases. This result is in agreement with those obtained from rheological and laser diffraction measurements because emulsions became more stable against creaming due to the combination of the increase of viscosity and the reduction of the droplet size.[26] It is important to note that destabilization by creaming could be visually observed for 1/2 emulsion after more than 40–45 days of aging time.

Taking into account that the emulsions were destabilized simultaneously by both processes, creaming and coalescence, the influence of Atlas™ G-5000/Atlox™ 4913 ratio in the global destabilization parameter, Turbiscan Stability Index, was studied. Table IV also shows the Turbiscan Stability Index (TSI) for

Table IV. Creaming Velocity (ω) and Turbiscan Stability Index at 60 days (TSI) for All Emulsions Studied

Emulsion	ω (%/day)	TSI_{60days}
3/0	0.019 ± 0.002	1.14 ± 0.11
2.5/0.5	0.048 ± 0.005	1.95 ± 0.16
2/1	0.098 ± 0.009	2.73 ± 0.19
1/2	0.283 ± 0.023	4.31 ± 0.33

60 days of aging time for all emulsions studied. 1/2 emulsion exhibited the highest value of TSI while the 3/0 emulsion showed the lowest. Therefore, it should be noted that the most stable emulsion (lowest values of TSI) is the formulation with 3 wt % of Atlas™ G-5000 (3/0). ANOVA test demonstrated that surfactant ratio had significant effect upon the physical stability of the emulsions.

CONCLUSIONS

Stable D-limonene-in-water emulsions were obtained formulated with mixtures of two copolymers as emulsifier and gellan gum by using a high-pressure homogenizer. All the emulsions prepared exhibited mechanical spectra typical of faintly structured materials. The mechanical spectra, flow curves, and mean droplet sizes were sensitive to the mass ratio of Atlas™ G-5000/Atlox™ 4913 copolymers and were consistent with the physical stability of D-limonene in water emulsions. Higher concentrations of Atlas™ G-5000 led to higher viscoelasticity, higher viscosity, higher yield stress, and lower mean droplet diameters. These results emphasize the relevant role played by the hydrophilic Atlas™ G-5000 copolymer, which promote steric interactions among limonene droplets, by means of a mechanism based on the competition to form hydrogen bonds with water in the continuous phase. All emulsions underwent a main destabilization process by creaming which was delayed as increase the Atlas™ G-5000/Atlox™ 4913 mass ratio.

ACKNOWLEDGMENTS

The financial support received (Project CTQ2011-27371) from the Spanish Ministerio de Economía y Competitividad and from the European Commission (FEDER Programme) is kindly acknowledged.

REFERENCES

1. McClements, D. J. *Rev. Food Sci.* **2007**, *47*, 611.
2. Dickinson, E.; Woskett, C. C. In Food Colloids; Bee, R. D, Richmond, P., Mingins, J., Eds.; Royal Society of Chemistry: London, **1989**, 74.
3. Callaway, T. R.; Carroll, J. A.; Arthington, J. D.; Edrington, T. S.; Anderson, R. C.; Ricke, S. C.; Nisbet, D. J. In Nutrients, Dietary Supplements, and Nutriceuticals: Cost Analysis Versus Clinical Benefits; Watson R.; Gerald J.; Preedy V. R., Eds.; Humana Press: New York, **2011**, 277.
4. García, M. C.; Alfaro, M. C.; Calero, N.; Muñoz, J. *Carbohydr. Polym.* **2014**, *105*, 177.
5. Trujillo-Cayado, L. A.; Ramírez, P.; Alfaro, M. C.; Ruíz, M.; Muñoz, J. *Colloid Surf. B: Biointerfaces* **2014**, *122*, 623.
6. Kerton, F. In Alternative Solvents for Green Chemistry; Kerton, F. M., Ed. Royal Society of Chemistry: Cambridge, **2009**, 1.
7. Pérez-Mosqueda, L. M.; Ramírez, P.; Trujillo-Cayado, L. A.; Santos, J.; Muñoz, J. *Colloid Surf. B: Biointerfaces* **2014**, *123*, 797.
8. Tadros, T. F. *Adv. Colloid Interface Sci.* **2009**, *147*, 281.
9. Sworn, G. In Xantham Gum, in Food Stabilisers, Thickeners and Gelling Agents; Imeson, A., Ed.; Wiley-Blackwell: Oxford, **2010**, 325.
10. García, M. C.; Alfaro, M. C.; Calero, N.; Muñoz, J. *Biochem. Eng. J.* **2011**, *55*, 73.
11. García, M. C.; Alfaro, M. C.; Muñoz, J. *J. Food Eng.* **2015**, *159*, 42.
12. García, M. C.; Alfaro, M. C.; Muñoz, J. *Colloid Surf. B: Biointerfaces* **2015**, *135*, 465.
13. Dickinson, E.; Goller, M. I.; Wedlock, D. *J. Colloids Surf. A: Physicochem. Eng. Aspect* **1993**, *75*, 195.
14. Schultz, S.; Wagner, G.; Urban, K.; Ulrich, J. *Chem. Eng. Technol.* **2004**, *27*, 361.
15. Urban, K.; Wagner, G.; Schaffner, D.; Röglin, D.; Ulrich, J. *Chem. Eng. Technol.* **2006**, *29*, 24.
16. Stang, M.; Schuchmann, H.; Schubert, H. *Eng. Life Sci.* **2001**, *1*, 151.
17. Pérez-Mosqueda, L. M.; Trujillo-Cayado, L. A.; Carrillo, F.; Ramírez, P.; Muñoz, J. *Colloid Surf. B: Biointerfaces* **2015**, *128*, 127.
18. Santos, J.; Trujillo-Cayado, L. A.; Calero, N.; Alfaro, M. C.; Muñoz, J. *Chem. Eng. Technol.* **2013**, *36*, 1883.
19. Ghannam, M. T.; Esmail, N. *J. Petrol. Sci. Eng.* **2005**, *47*, 105.
20. Jafari, S. M.; Beheshti, P.; Assadpoor, E. *J. Food Eng.* **2012**, *109*, 1.
21. Patel, D.; Ein-Mozaffari, F.; Mehvar, M. *Chem. Eng. Res. Des.* **2015**, *100*, 126.
22. Jafari, S. M.; He, Y.; Bhandari, B. *J. Food. Eng.* **2007**, *82*, 478.
23. Trujillo-Cayado, L. A.; Natera, A.; García, M. C.; Muñoz, J.; Alfaro, M. C. *Grasas Y Aceites* **2015**, *66*, e087.
24. Pal, R. *J. Colloid Interface Sci.* **2000**, *225*, 359.
25. Mengual, O.; Meunier, G.; Cayre, I.; Puech, K.; Snabre, P. *Colloids Surf. A: Physicochem. Eng.* **1999**, *152*, 111.
26. Santos, J.; Trujillo-Cayado, L. A.; Calero, N.; Muñoz, J. *AICHE J.* **2014**, *60*, 2644.
27. Reekmans, S. In Chemistry and Technology of Agrochemical Formulations; Knowles, D. A., Ed., Kluwer Academic Publishers: The Netherlands, **1998**, 179.